ACS OMEGA

http://pubs.acs.org/journal/acsodf

Article

Biobased Epoxy Composites Reinforced with Acetylated Corn Straw

Siyu Jiang, Chunhua Lou,* Yongli Zhou, Xiaohua Gu, and Xianzhi Kong*

Cite This: *ACS Omega* 2023, 8, 12644−12652

Read Online

ACCESS | Metrics & More | Article Recommendations

ABSTRACT: Corn straw/epoxy resin composites (CS/ECs) and maleic anhydride acetylated CS/ECs (MA-CS/ECs) were prepared through dry mixing and high-temperature curing. Corn straw is a kind of abundant, eco-friendly, and low-cost biomass material. Unmodified and modified corn straws were characterized using Fourier transform infrared spectroscopy, scanning electron microscopy (SEM), and X-ray photoelectron spectroscopy (XPS). The interfacial affinity of the composite was testified by the contact angle. The results of XPS and SEM demonstrated that maleic anhydride had been successfully bonded onto the structure of corn straw. Corn straw particle-reinforced epoxy resin composites were prepared using a casting and molding process. Results showed that the MA-CS/EC had better impact and flexural resistance than the unmodified corn straw/epoxy resin composites when the corn straw addition was 15 wt %. The result of the contact angle showed that the interfacial compatibility between composites is also stronger than that of CS/EC.

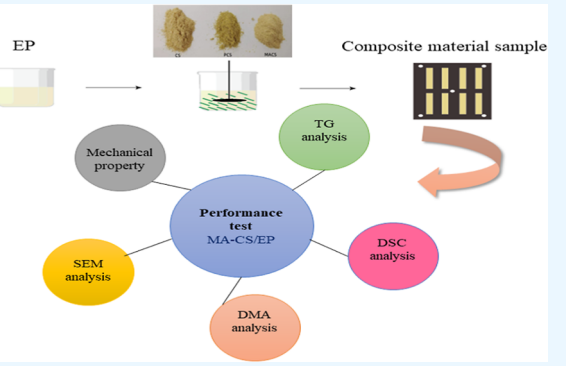

1. INTRODUCTION

Epoxy resin as a base material has high bond strength, good thermal stability, small curing shrinkage, good wear resistance, good dimensional stability, and easy processing. It has been widely used in adhesives, electronic instruments, aerospace, machinery, light industry, construction, paints, electrical and electronic insulation materials, and other fields.[1−3] However, the cured epoxy resin has fatigue, heat resistance, and poor impact resistance.[4,5] This drawback has limited the application of epoxy resins to a large extent. Therefore, toughening epoxy resin becomes a research focus.[6,7]

With the growth of the bioeconomy and awareness of ecological conservation in recent years, an increasing number of people are seeking biomass-derived molecules and materials with new functions, enhanced properties, and a low carbon footprint to be used in different fields.[8,9] Compared with traditional reinforcement materials, biomass materials are abundant, eco-friendly, and low-cost; their mechanical and physical properties can also be further improved and perfected through modification.[10,11] Therefore, toughening epoxy resins by biomass materials has been recognized as an important way to expand their application.

The main biomass materials commonly used in resin-based composite reinforcement are straw, stalk, walnut shells, and wood and its residues.[12] The relatively weak mechanical properties compared with synthetic fibers are the main drawback of biomass-reinforced composites; thus, it limits the scope of practical applications of biomass composites to some extent.[13] The reason is the presence of a large number of polar hydroxyl groups in the molecular structure of biomass materials, which makes them prone to hydrophilicity and agglomeration. This inclination ultimately results in relatively poor interfacial compatibility between the filler and the nonpolar polymer matrix. Thus, their scope of application in biomass-reinforced composites is limited. Therefore, biomass materials need to be modified by suitable treatments to improve the interfacial compatibility between the filler and the reinforced material and enhance the mechanical properties of the composites.[14]

Research and development of low cost, simple, and efficient biomass material modification solutions can effectively expand the application areas of biomass filler-reinforced composites. The combination of biomass materials, which are highly hydrophilic, and matrix polymers, which are nonpolar and hydrophobic, leads to poor interfacial bonding, mechanical properties, and hygrothermal durability of biomass composites; composites made from unmodified biomass fillers also have a large number of voids and are highly susceptible to stress concentration.[15,16] These shortcomings of biomass composites limit their scope for practical applications; thus, the modification of biomass materials has great research importance.[17] At present, the main methods of processing biomass materials for high-performance modification are

Received: October 31, 2022
Accepted: March 20, 2023
Published: March 29, 2023

physical, chemical, biological, and combined methods. Some of the hydroxyl groups (—OOR) under certain conditions due to the large number of hydroxyl groups on the surface of biomass materials, and these ester groups are transformed into the corresponding acylates. Mahesha et al.[18] found that the tensile strength of acetylated hemp fiber-reinforced composites was 15 times higher than that of untreated fiber-reinforced composites, and the flexural modulus and strength were also higher than those of unacetylated materials. Shah et al.[19] used catechu (biomass) pellets to reinforce epoxy resins, which increased the toughness and impact strength of the composites by 52 and 94%, respectively, when catechu was added at 1 wt %. This study aims to investigate the interfacial affinity, mechanical, and thermal properties of Maleic anhydride-modified corn straw particle-reinforced epoxy resin matrix biocomposites.

2. EXPERIMENTAL SECTION

2.1. Materials. Epoxy resin (E-51) was purchased from Baling Branch of Sinopec. Corn straw (CS) was obtained from suburb of Qiqihar City, Heilongjiang Province. 2-Methylimidazole and Acetone were purchased from Tianjin Kermel chemical reagent development center. Maleic anhydride (MA) was purchased from Tianjin Windship Chemical Reagent Technology Co. *N*,*N*-Dimethylformamide (DMF) was purchased from Fuchen (Tianjin) Chemical Reagent Co. Sodium bicarbonate (K_2CO_3) was purchased from Tianjin Comio Chemical Reagent Development Centre.

2.2. Materials Characterization and Mechanical Testing. The Au-sputter-coated cross section of the cured epoxy coupons after impact tests was used for surface morphology analysis by scanning electron microscopy (SEM) (S-3400, Japan)."

Potassium bromide pressings were made and samples were measured in the frequency range of 4000−500 cm^{-1} using online Fourier transform infrared (FTIR) optical fiber detection system (Frontier, USA).

Samples were dried at 70 °C for 8 h, ground for 3 min, quickly pressed, and fixed on slides with double-sided tape. The samples were tested using contact angle measuring instrument (KRUSS-DSA25, Germany) at 25 °C with distilled water at three different regional locations, each time with a volume of 5 μL, and averaged.

The sample needs to be paved before the test, and the data after the test is processed by XPSPEAK4.1 software for peak splitting and spectral analysis.

The mass of the specimen in this experiment was 6−10 mg. The TGA method was used for the determination.

Single suspension beam mode with 1 Hz, specimen size 25 mm × 12 mm × 3 mm, air atmosphere, heating rate 5 K/min, and test temperature 40−200 °C.

An aluminum crucible was placed in a cuvette with a sample of about 8 mg; the temperature of the system was increased from 25 to 220 °C at a constant heating rate of 10 °C/min and the heat of reaction of the curing process was measured as ΔH.

In accordance with ISO 179-1:2000, the impact property was conducted on the charpy impact tester (GT-7045-HMH, China) at room temperature. The dimension of specimens was 80 mm × 10 mm × 4 mm with no notches.

The tensile property was operated on the electronic universal testing machine (WSM-20KN, China) according to ISO 527:1993 with the loading speed is 2 mm/min at room temperature under the load of 20 kN.

The flexural property was manipulated on the electronic universal testing machine (WSM-20KN, China) according to ISO 178:1993 with the loading speed is 2 mm/min at room temperature under the load of 500 N.

Cut the straw into pieces and grind with a grinder (200T, China) three times for 2 min each time. Sift. Select 80−120 for retention.

Drying experiments were operated in an Air Blast Drying Box (DHG-9140S, China).

2.3. Preparation of Samples. *2.3.1. Corn Straw Powder Preparation.* The raw CS was stirred in a water bath at 80 °C for 2 h. Washed and repeated three times. The wet raw CS was rinsed with distilled water, blast-dried at 80 °C for 24 h, and shortened to about 2 cm. The short CS was crushed with the grinder, and the ground raw CS powder was sieved through 80−120 mesh for further wash with a mixture of acetone and ethanol in 2:1 volume ratio. In a typical experiment, 5 g of raw CS power was placed in 100 g of acetone/ethanol mixture in a beaker and sonicated in an ultrasonic cleaner at 60 °C for 3 h. The mixture was then vacuum-filtrated, and the solid sample was washed with anhydrous ethanol and then distilled water three times each. The powder sample normal dry at 80 °C for 24 h detected and named pre-treated corn straw (PCS).

2.3.2. Acetylation of PCS. 5.0 g of PCS in 50 mL of DMF was stirred in a 250 mL beaker for 30 min and then sonicated for 2 h. The mixture was transferred into a 250 mL round-bottom flask together with 0.25 g of K_2CO_3. A solution of 40 g of MA in 100 mL of DMF in a pressure equalizing dropping funnel was slowly dropped into the flask. After the reaction completed over 1 h, the solid was separated from the reaction mixture through vacuum filtration and further purified in a Soxhlet extractor with DMF for 3 h. The purified product was blast-dried at 120 °C for 24 h. The product was placed in a sealed bag and set aside. The experiment was repeated to obtain MA-CS.

After the corn stalk is ground into powder, the surface is rough, as shown in Figure 1 CS. After pretreatment, some soluble organic compounds were dissolved by the solvent and the surface became loose, as shown in Figure 1 PCS. After chemical modification, the surface structure of the modified corn stalk powder changed, making the color lighter and more delicate, as shown in Figure 1 MA-CS.

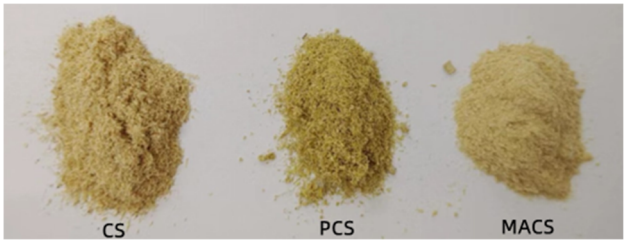

Figure 1. Untreated and chemically treated corn straw particles.

2.3.3. Preparation of Epoxy Resin Composite with Acetylated Corn Straw. Three portions of 50 g E-51 each were placed in disposable cups and marked as 1, 2, and 3, respectively. A total of 15% mass fraction of raw CS and MA-CS were placed in 1 and 2 plastic cups, respectively. They were stirred well, placed in an oven at 60 °C for 20 min preheating, removed, and continuously stirred for 15 min. A total of 4 wt % of 2-MI was added to all three plastic cups, which were mixed and stirred for 30 min until homogeneous. Finally, the epoxy

https://doi.org/10.1021/acsomega.2c06947
ACS Omega 2023, 8, 12644−12652

mixture was poured into the mold and cured for 1 h at 80 °C preheated and then for 2 h at 113 °C. The cured complex is noted as CS/EC and MA-CS/EC.

3. RESULTS AND DISCUSSION

3.1. Fourier Infrared Spectroscopy Analysis. FTIR analysis was conducted out on corn straw before and after modification. As shown in Figure 2, the wavenumber at 3428

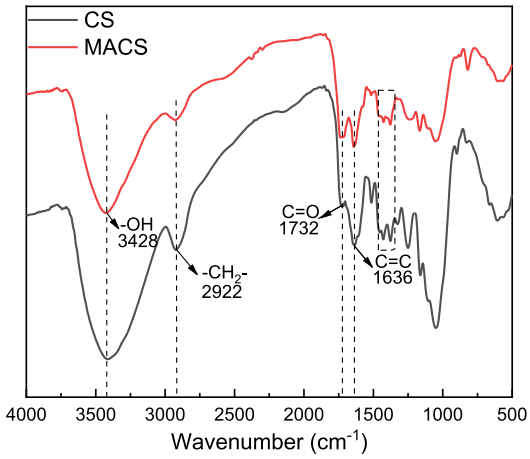

Figure 2. Infrared spectra of corn straw before and after modification.

cm^{-1} is the stretching vibration peak of the hydroxyl group (−OH), asymmetric stretching vibration peak of $-CH_2$ at 2922 cm^{-1}, the broader absorption peak at 1636 cm^{-1} is the stretching vibration of the double bond (−C═C−) and the skeleton vibration of the aromatic benzene ring in lignin, and the absorption peak near 1400 cm^{-1} is the skeleton vibration of the aromatic ring in lignin vibrations.[20] The absorption peak at 1732 cm^{-1} clearly changes to the characteristic C═O stretching vibration peak, and no stretching vibration peak of C═O is observed at 1850−1750 cm^{-1}. A review of the data shows[21] that the groups with wavenumbers in the range of 1740−1710 cm^{-1} are noncyclic esters, which indicates that MA has been successfully bonded onto CS and the modified corn straw does not contain unreacted anhydride; after modification by MA, the hydrophilic group hydroxyl (−OH) on the surface of the corn straw is reduced and carbonyl (C═O) and ester groups (O═C−O) are present in large numbers, which demonstrates that ester functional groups have been successfully introduced.

3.2. X-ray Photoelectron Spectroscopy Analysis. XPS was used to characterize the chemical valence state and the relative content in the samples before and after corn straw modification. The C 1s peak of carbon was used to correct for the electron binding energy. Figure 3 shows the full XPS spectra of CS and MA-CS (Figure 4a,b) and the C 1s spectra after Gaussian curve fitting and deconvolution (Figure 4c,d), where the C 1s XPS spectra of corn straw fibers have four typical carbon bond forms of plant fibers (C1: C═C, C−C, C−H; C2: C−O; C3: C═O, O−C−O; and C4: O−C═O).[22] As shown in Figure 4c,d, four C contents of the corn straw also change significantly after treatment with maleic anhydride. In the C composition, the reduced C1 content is due to the destruction of lignin and extractable waxes in the straw fiber by MA during the esterification reaction. C2 is mainly derived from the hydroxyl group of the fiber, and its relative content is significantly reduced by the involvement of the hydroxyl group in the reaction. Meanwhile, the increased content of C3 and C4 is caused by the conversion of most of the hydroxyl groups in the amorphous and disrupted crystalline regions of the fiber surface into ester groups (O═C−O), which also indicates the introduction of ester groups to the fiber surface.[23,24]

3.3. Static Contact Angle Analysis. The contact angle test plots of water drops on the CS and MA-CS surfaces at different times are shown in Figure 4. As shown in Figure 4a−f, CS fibers are very hydrophilic and absorb water nearly instantly. Meanwhile, MA-CS is somewhat hydrophobic. The contact angles are shown in Table 1, with CS having a contact angle of 19.1° at 0 s and 15.83° at 30 s, while the MA-CS has a contact angle of 119.05° at 0 s, 104.45° at 30 s, and 99.45° at 60 s for water droplets. This result shows that the modified fiber surface has good hydrophobic properties due to the substitution of hydrophilic hydroxyl groups on the surface of the corn straw by ester groups, which forms hydrophobic esterification groups.

3.4. Thermogravimetric Analysis of MA-CS/EC. The thermal degradation process of the epoxy composites was evaluated using the TGA technique. The curves of TG and DTG for E-51, CS/EC-15 and MA-CS/EC-15 under a nitrogen atmosphere are shown in Figure 5, and the thermal degradation parameters are shown in Table 2. The initial decomposition temperature of each composites changes significantly with the addition of CS and MA-CS.

As shown in Figure 5, E-51 loses very little weight below 300 °C, which is probably due to the decomposition of water or small organic molecules. At 300 °C, the movement of the molecular chain segments of the epoxy resin material intensifies, and some groups with poor thermal stability begin to be thermally decomposed. The force between the chain segments begins to be unable to maintain the stability of the whole molecular chain with the rise of temperature, and fractures occur between the chain segments. When the temperature reaches about 400 °C, the internal structure of the material is destroyed and a large number of thermal decomposition occurs. At 500 °C, the thermal decomposition is completed. Compared with the $T_{d5\%}$, $T_{d50\%}$, and T_{max} of the pure epoxy resin, those of CS/EC-15 composites are 278, 427, and 459 °C, respectively. Its maximum weight loss peak is at 422 °C, which is lower than that of the pure epoxy resin at 429 °C. This finding may be due to the poor interfacial bonding between CS and epoxy resin, which makes some of the hemicellulose in CS start to thermally decompose at a lower temperature (215 °C) and began to lose a lot of weight at 330−500 °C. At this time, the CS in the cellulose and lignin begin to thermally decompose,[25] while the polymer matrix in the molecular chain segments in the higher temperature is heated and has a large number of fracture decomposition. At 500−800 °C, material thermal decomposition stops. The $T_{d5\%}$, $T_{d50\%}$, and T_{max} of MA-CS/EC-15 are 369, 443, and 474 °C, respectively. The maximum weight loss peak appeared at 448 °C, which moves toward higher temperature than the pure epoxy resin. Therefore, the modification of MA improves the thermal stability of CS, and the thermal stability performance of the epoxy resin composites enhanced by MA-CS is also improved to a certain extent. This result is due to the formation of a homogeneous and stable structure between MA-CS and the epoxy resin matrix. At around 300 °C, MA-CS is thermally decomposed into carboxylic acid, which promotes the dehydration of E-51 into carbon. The resulting carbon

https://doi.org/10.1021/acsomega.2c06947
ACS Omega 2023, 8, 12644−12652

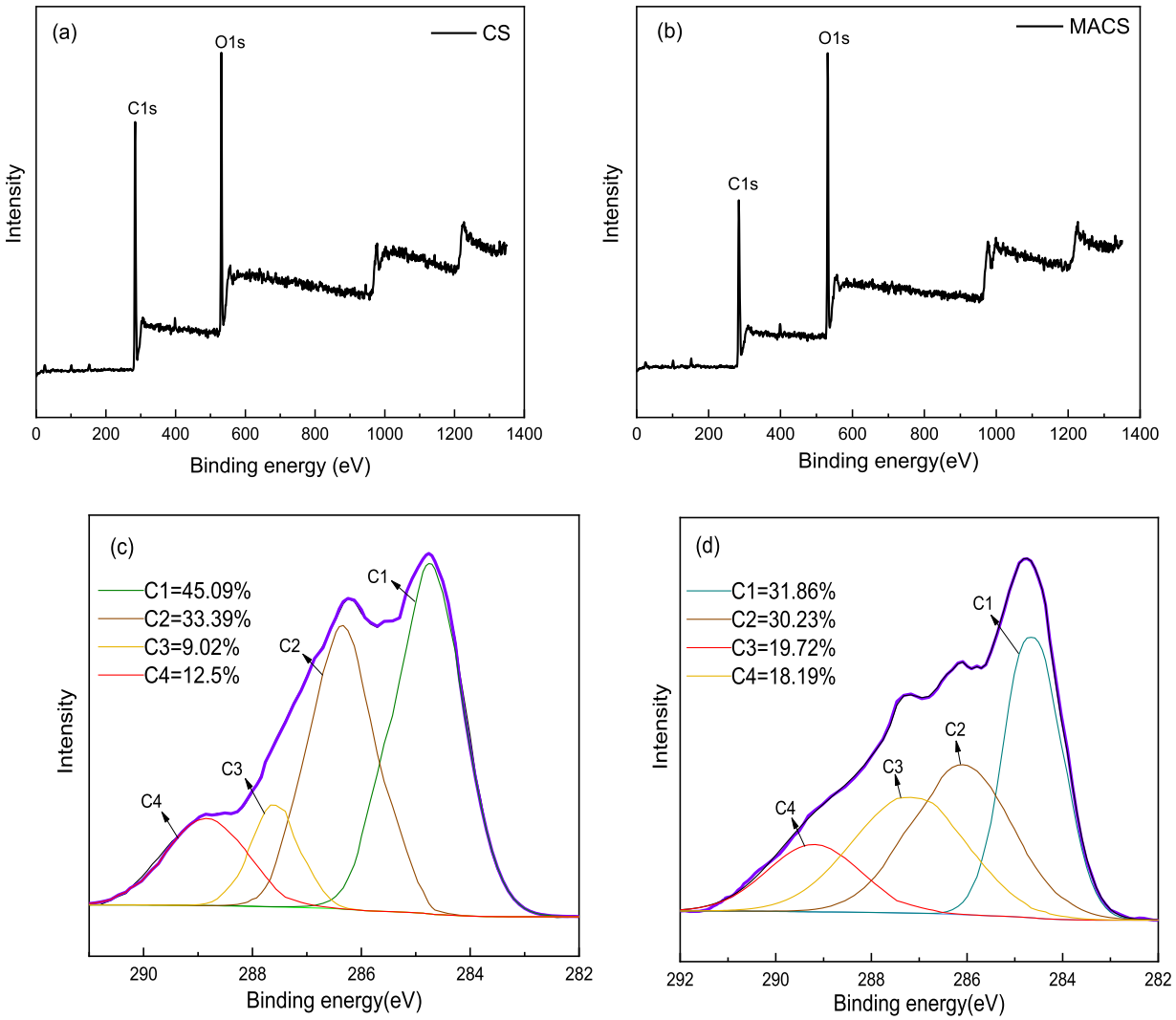

Figure 3. XPS scan of corn straw before and after modification. (a) XPS wide scan of CS; (b) XPS wide scan of MACS; (c) C1 unstack diagram of CS; and (d) C1 unstack diagram of MACS.

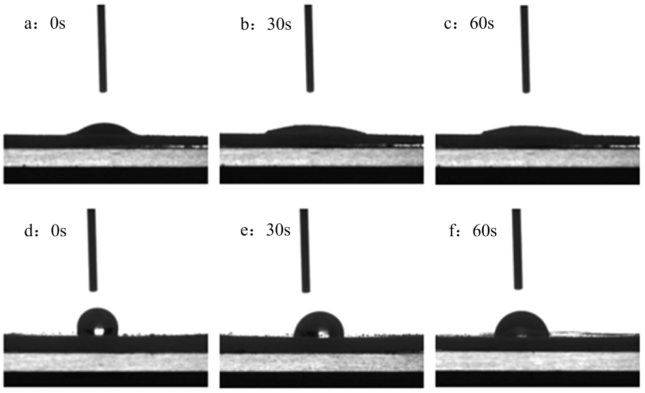

Figure 4. Static contact angle test diagram of corn straw before and after modification.

layer acts as a heat insulator as the temperature rises, and the degradation rate of the MA-CS system begins to decrease until the degradation is complete. The chemical bonds formed by MA-CS with the epoxy resin matrix may contribute to the thermal stability of the material. Therefore, MA-CS can be added to some resins that require high-temperature curing.

Table 1. Contact Angle Measurements of a Water Droplet on the Surface of CS and MACS

	contact angle measurements/°		
samples	0 s	30 s	60 s
CS	19.1	0	0
MACS	119.05	104.45	99.45

As shown in Table 2, the amount of residual carbon in the system with the addition of CS and MA-CS is much higher than that of pure EP. A total of 29% of the residual carbon is increased for CS/EC-15 and 38% for MA-CS/EC-15. Therefore, the addition of CS and MA-CS can promote the formation of a dense carbon layer, which is a protective carbon layer that prevents the penetration of oxygen and heat and inhibits the mass loss. This protective carbon layer prevents the penetration of oxygen and heat and suppresses the rate of mass loss, which delay the thermal degradation process and greatly enhance the flame retardancy of EP. This finding is in good agreement with the flame-retardant mechanism of the condensed phase.[26]

3.5. Differential Scanning Calorimetry Analysis of MA-CS/EC. The DSC curves for the different systems of epoxy

https://doi.org/10.1021/acsomega.2c06947
ACS Omega 2023, 8, 12644−12652

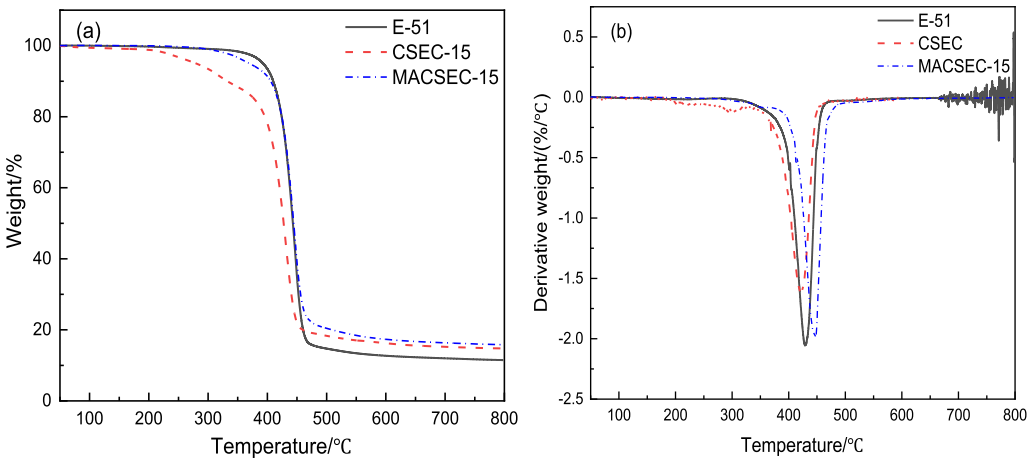

Figure 5. (a) TG and (b) DTG curves of pure E-51 and composites.

Table 2. Thermal Degradation Parameters of Different Systems[a]

sample	$T_{d5\%}$	$T_{d50\%}$	T_{max}	char residue (%)
E-51	390	443	468	11.49
CSEC-15	278	427	459	14.79
MACSEC-15	369	443	474	15.86

[a] $T_{d5\%}$ and $T_{d50\%}$ are the corresponding decomposition temperatures for 5 and 50% weight loss, respectively; T_{max} is the temperature corresponding to the maximum thermal decomposition rate.

composites after curing at a temperature rise rate of 10 °C/min are shown in Figure 6. The trend is the same for each system,

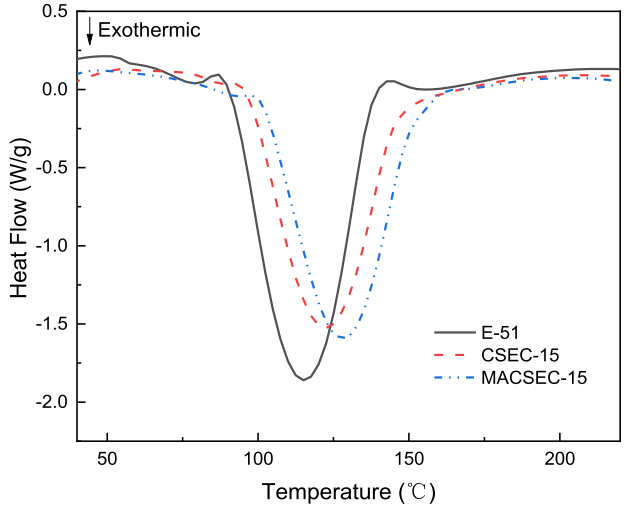

Figure 6. DSC thermograms corresponding to the dynamic curing of the studied resins at 10 °C/min.

that is, both have two exothermic peaks. Farkas and Strohm[27,28] showed that the reaction between the imidazole ring and the epoxide group involves two steps: the small peak in front is the addition reaction between the N atom in the imidazole and the epoxide group, and the addition reaction is the induction period of the spatial polymerization. After the induction period, the negative ion of the oxane is formed by the addition reaction and the epoxide. At the end of the induction period, the polymerization reaction between the oxyalkane anion and the epoxide group begins, followed by a large peak at high temperature.[29] With the addition of CS and MA-CS, the peaks move toward higher temperatures, which indicates an increased degree of curing; the restriction of movement of the polymer chains is the main factor causing the peaks to move toward higher temperatures.[30] MA-CS in MA-CS/EC-15 has better dispersion in the epoxy matrix, stronger interfacial bonding with E-51, and limits the movement of the polymer chains more effectively than that in CS/EC-15.[31]

3.6. Analysis of the Mechanical Properties of MA-CS/EC. The mechanical properties of the composites were investigated to analyze the toughening effect of different additions of CS and MA-CS on the epoxy resin. The mechanical property test results of each system are shown in Figures 7–9.

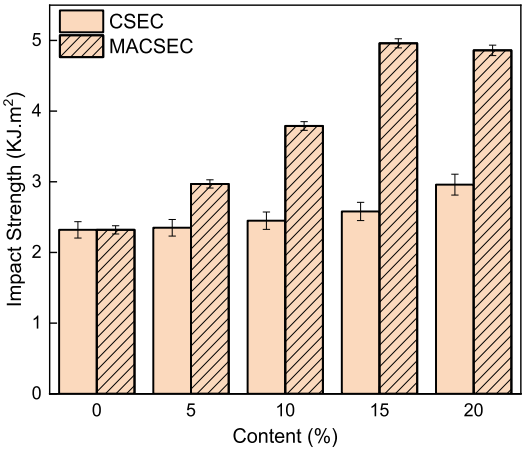

Figure 7. Impact strength diagrams of composites.

As shown in Figure 7, the impact strength of the composite increases and then decreases with the addition of MA-CS to the epoxy resin. It reaches its highest value at 15 wt % addition. The maximum impact strength of the composite is 4.96 KJ/m^2 when 15 wt % MA-CS is added. It is 114% higher than that of pure epoxy and 92.2% higher than that of 15 wt % CS. Notably, the addition of MA-CS can effectively improve the impact resistance of epoxy resins. The reasons can be attributed to the following two aspects: (1) MA-CS has a reduced surface polarity, is more compatible with the pure epoxy resin matrix, and acts as a buffer phase in the composite

https://doi.org/10.1021/acsomega.2c06947
ACS Omega 2023, 8, 12644−12652

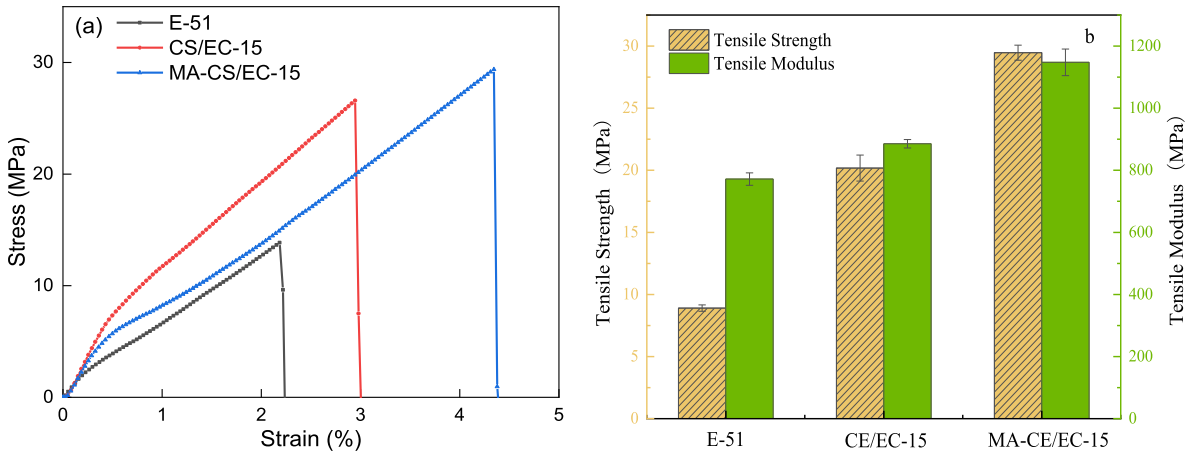

Figure 8. (a) Tensile stress−strain curves of the composites; (b) tensile strength and modulus diagrams of the composites.

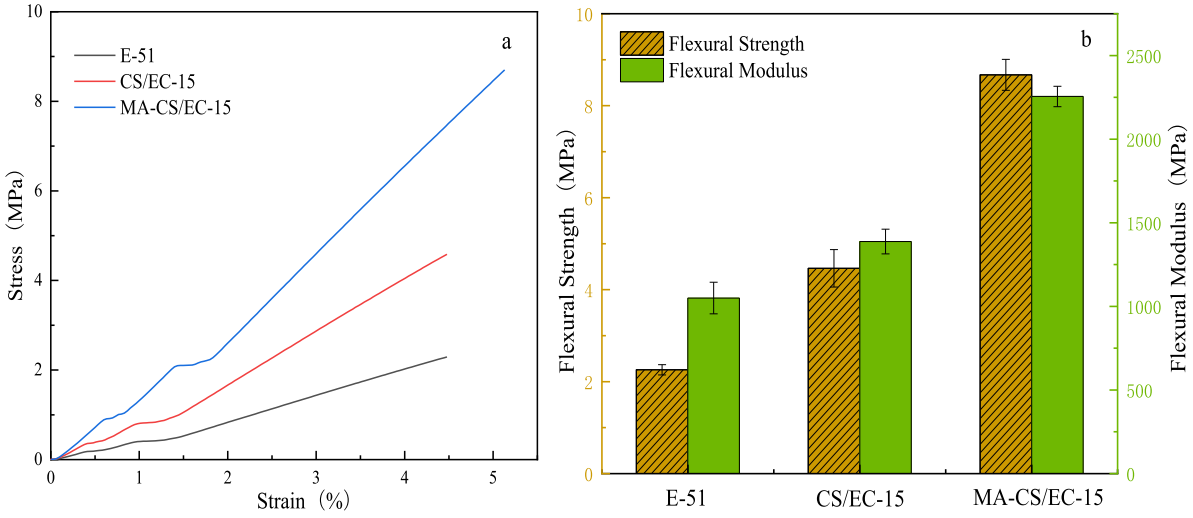

Figure 9. (a) Flexural stress−strain curves of the composites; (b) flexural strength and modulus diagrams of the composites.

to absorb impact energy; (2) MA-CS is bonded to the epoxy resin by chemical bonding, which can further improve the impact capacity of MA-CS in the composite. Thus, the impact strength of MA-CS/EC-15 can be improved.

The tensile stress−strain curves of the composites filled with different fillers are shown in Figure 8a. The graph shows a significant improvement in the toughness of the composites compared with the epoxy resin. Meanwhile, the epoxy resin exhibits a brittle fracture mode, and the corn straw-reinforced composites exhibit a ductile fracture yield point characteristic.[32] Figure 8b shows the tensile strength and tensile modulus of the composites with different fillers. The tensile strengths of CS/EC-15 and MA-CS/EC-15 increased by 94.81 and 115.29% compared with that of pure epoxy resin, which implies that the reinforcing phase effectively increases the stiffness of the composites; the tensile moduli of CS/ES-15 and MA-CS/EC-15 increased by 14.80 and 48.77%, which suggests that the MA-CS/EC-15 is more rigid than the CS/EC-15.[33] In summary, the straw has an enhanced toughening effect on epoxy resins.

Figure 9a shows the flexural stress−strain curves of the composites with different filler fillers. The curves indicate that the strength and toughness of the composites are increased to different degrees. According to the literature, the improvement in the toughness of polymer composites may be dependent on not only the better dispersion of the particles in the polymer[34] but also the formation of strong interactions between the reinforcing material and the polymer.[35] The physical and chemical bonding of the MA-modified CS with E-51 is more likely than that of the CS, which allows for better interaction and distribution in the mixed matrix. Thus, it can withstand greater loads when bonded to the interface between the matrix, which achieves strengthening and toughening. Figure 9b shows the flexural strength and modulus of the composites with different filler fillers. The flexural strength and modulus of the CS/EC-15 increased by 96.48 and 32.19% compared with those of the pure epoxy resin; the flexural strength and modulus of the MA-CS/EC-15 increased by 281.84 and 121.76%. This result is due to the increased functional groups reacting with the epoxy resin on the surface of MA-CS, which results in a higher cross-link density. This condition reduces the motility between the molecular chain segments. Ultimately, the MA-CS/EC-15 has a greater increase in flexural strength than CS/EC-15. The modulus of the composite has increased more than CS/EC-15, while the load can be transmitted through the straw particles, which disperses the stresses acting on the matrix resin. Therefore, the flexural strength of the resin is increased.

3.7. Dynamic Mechanical Thermal Analysis of MA-CS/EC. Dynamic mechanical thermal analysis is commonly used to

https://doi.org/10.1021/acsomega.2c06947
ACS Omega 2023, 8, 12644−12652

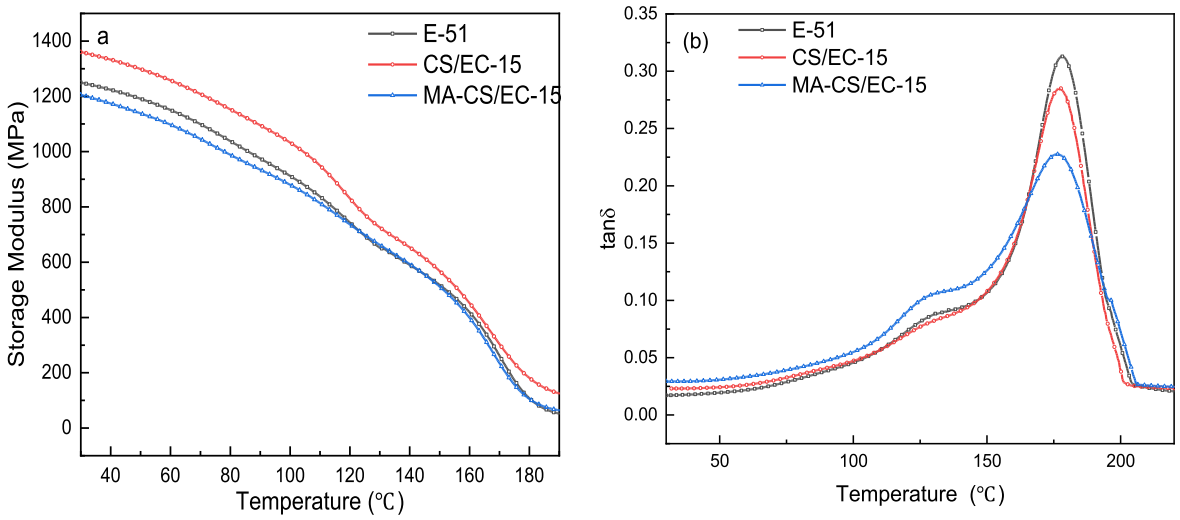

Figure 10. Curves of storage modulus and loss modulus of the composites with temperature. (a) Changes of energy storage modulus at different temperatures, (b) tan δ at different temperatures.

study the mechanical properties and viscoelastic behavior of polymers and polymer-based materials, such as epoxy composites, as a function of temperature, frequency, and time.[36,37] As shown in Figure 10a, the addition of CS increases the energy storage modulus of the composite, while MA-CS decreases the energy storage modulus of the composite. The reason may be that the modification by MA reduces the stiffness of the straw and increases the flexibility of the straw particles to a certain extent.[38] Moreover, the more flexible straw particles can absorb some of the energy by moving by themselves in the interfacial region. Thus, the stiffness of the composite is decreased. This trend is consistent with that of the energy storage modulus of the composites. Figure 10b shows the trend of tan δ peak and T_g with temperature for the different filler composites. As observed, the T_g of the composites is constant and the tan δ peak is lower for CS and MA-CS than for the pure epoxy resin, which means that CS and MA-CS enhance the toughness of the epoxy resin. Meanwhile, the toughness of MA-CS/EC-15 is stronger than that of CS/EC-15 because the MA surface treatment CS improves the interfacial adhesion of the straw particle-epoxy resin matrix. The stronger interfacial bonding of MA-CS to the epoxy matrix limits the activity of MA-CS during stress transfer, which reduces the loss factor (glassy state) of the material.[39−41] This result is consistent with the tensile properties of the composite.

3.8. Micro Morphology Analysis. SEM and EDX analyses were conducted before and after modification of the corn straw, as shown in Figure 11, to evaluate the chemical changes in the surface composition before and after CS modification. Figure 11a shows the SEM micrographs of CS. The surface of the corn straw before modification is smooth, with a relatively dense structure and clearly fibrous appearance. Figure 11b shows the SEM micrograph of MA-CS. The modified straw has lost the morphology of the original straw. It now shows a wrinkled and uneven surface, as well as deep and shallow grooves, which facilitate the formation of a hydrophobic surface. The increased surface roughness also facilitates better compatibility with the epoxy resin.

The elemental analysis data are presented in Table 3, and they were obtained from the SEM micrographs of the CS and MA-CS samples. The elemental analysis data are presented in

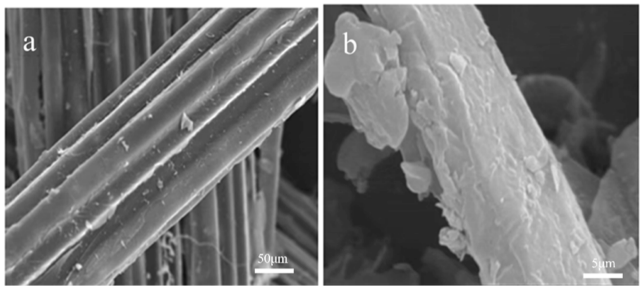

Figure 11. SEM images of corn straw before and after modification. (a) The corn straw was analyzed by SEM before modification, (b) SEM analysis of modified corn straw.

Table 3. EDX Date of CS/MA-CS Samples

element	C/wt %	O/wt %	total/wt %
CS	44.893	55.107	100.000
MACS	36.818	63.182	100.000

Table 3, and they were obtained from SEM micrographs of the CS and MA-CS samples (as shown) in the areas indicated by the red boxes. The EDX spectrum of each sample is located below the SEM micrograph in the figure. As shown in Table 1 and the graphs, the oxygen content of MA-CS shows an increasing trend compared with CS. Therefore, MA undergoes an esterification reaction with the hydroxyl groups on the surface of CS.

As shown in Table 3, the C and O compositions of the CS surface change before and after modification. Before modification, the C content of the CS surface is 44.89%, the O content is 55.11%, and the O/C ratio is 1.23. After modification by MA, the C content of the CS surface is 36.82%, the O content is 63.18%, and the O/C ratio is 1.72. This finding indicates that the MA-modified corn straw has successfully introduced ester groups to increase the O/C ratio of the surface.

The impact cross-sectional morphology of MA-CS/EC-15 with optimum mechanical properties was observed by SEM to study the interfacial interaction between it and E-51 and analyze the mechanism of MA-CS toughening epoxy resin. The SEM photos are shown in Figure 12. The figure shows that the

https://doi.org/10.1021/acsomega.2c06947
ACS Omega 2023, 8, 12644−12652

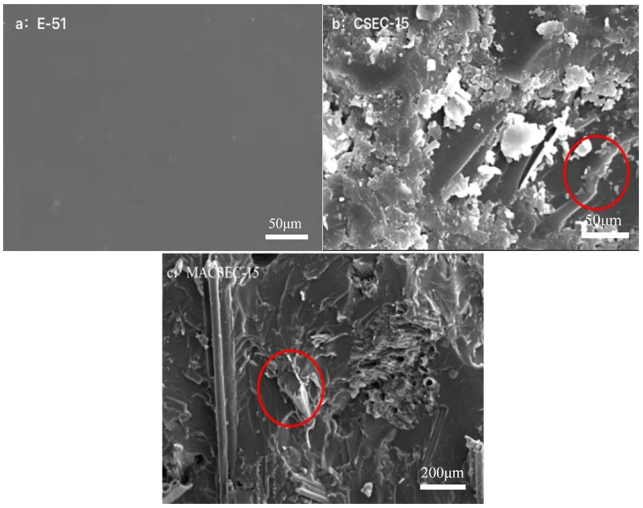

Figure 12. Impact fracture scans of composites with different fillers.

pure epoxy resin section is flat and smooth, which is typical of brittle fracture (Figure 12a). After adding CS, the section of CS/EC-15 (Figure 12b) appears rough and the folds are obviously increased. CS is observed embedded in the epoxy resin in the section, but the phase interface between the two phases is obviously present, which indicates that the compatibility between CS and E-51 is poor. However, CS can still act as a buffer energy segment, and CS can absorb part of the energy when the CS/EC-15 is impacted. This condition allows the impact strength of the composite to be enhanced. Compared with the impact section of the CS/EC-15, that of the MA-CS/EC-15 (Figure 12c) is rougher and has increased folds and irregular orientation. MA-CS appears in the impact section of the epoxy composite, and no obvious interface exists between the two, which implies that the interfacial force of MA-CS in the matrix can be enhanced through chemical bonding. At the same time, torn and disconnected MA-CS is found in the cross-sectional morphology, which confirms that MA-CS is torn and damaged when the composite is impacted. Thus, most of the energy is absorbed when the composite is impacted, which further enhances the toughness of the composite and improves the mechanical properties of the composite. Thus, MA-CS/EC-15 possessed better mechanical properties than E-51 and CS/EC-15.

4. CONCLUSIONS

In this work, a series of epoxy composites (CS/EC and MA-CS/EC) were fabricated using CS and MA-CS. The mass fraction of straw filler in these composites ranged from 0 to 20 wt %, with the final confirmation that the best performance of the epoxy composites was achieved at an addition level of 15 wt %. The focus of this study was to analyze the tensile mechanical, flexural mechanical, and impact properties of the composites and determine whether corn straw could toughen and strengthen the epoxy matrix. The results showed that the flexural modulus and strength of the MA-CS/EC increased by 61.3 and 64.4% compared with those of CS/EC at an addition level of 15 wt %. Meanwhile, the tensile modulus and strength decreased by 11.2 and 20.0%, and the impact strength increased by 92.2%. Dynamic mechanical thermal analysis further showed that corn straw had a toughening and a strengthening effect on the epoxy resin composites. Thermogravimetric analysis showed that the addition of CS and MA-CS promoted the formation of a dense carbon layer, which enhanced the thermal stability of the composites and greatly improved the flame retardancy of the epoxy resin composites.

AUTHOR INFORMATION

Corresponding Authors

Chunhua Lou − *College of Chemistry and Chemical Engineering, Qiqihar University, Qiqihar 161006, China; School of Energy and Building Environment, Guilin University of Aerospace Technology, Guilin 541004, China;* orcid.org/0000-0003-0595-8704; Email: chunhualou@163.com

Xianzhi Kong − *Institute of Petrochemistry, Heilongjiang Academy of Sciences, Harbin 150040, China;* Email: kongxianzhi2013@163.com

Authors

Siyu Jiang − *College of Chemistry and Chemical Engineering, Qiqihar University, Qiqihar 161006, China*

Yongli Zhou − *College of Chemistry and Chemical Engineering, Qiqihar University, Qiqihar 161006, China*

Xiaohua Gu − *School of Energy and Building Environment, Guilin University of Aerospace Technology, Guilin 541004, China*

Complete contact information is available at: https://pubs.acs.org/10.1021/acsomega.2c06947

Notes

The authors declare no competing financial interest.

ACKNOWLEDGMENTS

This work was supported by the Science and Technology Department of Heilongjiang Province [grant number E2018058]; the Education Department of Heilongjiang Province [grant numbers YSTSXK201861 and 135309437]; and the Heilongjiang Provincial Key Laboratory of Polymeric Composition Materials [grant number CLKFKT2021B8].

REFERENCES

(1) Kong, X. Z.; Xu, Z. F.; Guan, L. Z.; Di, M. W. Study on polyblending epoxy resin adhesive with lignin I-curing temperature. *Int. J. Adhesion Adhes.* **2014**, *48*, 75−79.

(2) Garea, S. A.; Corbu, A. C.; Deleanu, C.; Iovu, H. Determination of the epoxide equivalent weight (EEW) of epoxy resins with different chemical structure and functionality using GPC and ^{1}H-NMR. *Polym. Test.* **2006**, *25*, 107−113.

(3) Kosbar, L. L.; Gelorme, J. D.; Japp, R. M.; Fotorny, W. T. Introducing biobased materials into the electronics industry. *J. Ind. Ecol.* **2000**, *4*, 93−105.

(4) Liu, Y. L. Flame-retardant epoxy resins from novel phosphorus-containing novolac. *Polymer* **2001**, *42*, 3445−3454.

(5) Levchik, S. V.; Weil, E. D. Thermal decomposition, combustion and flame-retardancy of epoxy resins - a review of the recent literature. *Polym. Int.* **2004**, *53*, 1901−1929.

(6) Venkatesan, G.; Jithin, P. R.; Rajan, T. V.; Pitchan, M. K.; Bhowmik, S.; Rane, R.; Mukherjee, S. Effect of titanium nitride coating for improvement of fire resistivity of polymer composites for aerospace application. *P. I. Mech. Eng. G-J. Aer.* **2018**, *232*, 1692−1703.

(7) Mohan, P. A critical review: the modification, properties, and applications of epoxy resins. *Polym.-Plast. Technol.* **2013**, *52*, 107−125.

(8) Gandini, A. The irruption of polymers from renewable resources on the scene of macromolecular science and technology. *Green Chem.* **2011**, *13*, 1061−1083.

https://doi.org/10.1021/acsomega.2c06947
ACS Omega 2023, 8, 12644−12652

(9) Tuck, C. O.; Perez, E.; Horvath, I. T.; Sheldon, R. A.; Poliakoff, M. Valorization of biomass: deriving more value from waste. *Science* **2012**, *337*, 695−699.
(10) Chonkaew, W.; Sombatsompop, N.; Brostow, W. High impact strength and low wear of epoxy modified by a combination of liquid carboxyl terminated poly (butadiene-co-acrylonitrile) rubber and organoclay. *Eur. Polym. J.* **2013**, *49*, 1461−1470.
(11) Jayan, J. S.; Saritha, A.; Joseph, K. Innovative materials of this era for toughening the epoxy matrix: a review. *Polym. Composite.* **2018**, *39*, E1959−E1986.
(12) Faruk, O.; Bledzki, A. K.; Fink, H. P.; Sain, M. Biocomposites reinforced with natural fibers: 2000−2010. *Prog. Polym. Sci.* **2012**, *37*, 1552−1596.
(13) La Mantia, F. P.; Morreale, M. Green composites: A brief review. *Composites, Part A* **2011**, *42*, 579−588.
(14) Rout, J.; Misra, M.; Tripathy, S. S.; Nayak, S. K.; Mohanty, A. K. Novel eco-friendly biodegradable coir-polyester amide biocomposites: Fabrication and properties evaluation. *Polym. Compos.* **2001**, *22*, 770−778.
(15) Nunez, A. J.; Kenny, J. M.; Reboredo, M. M.; Aranguren, M. I.; Marcovich, N. E. Thermal and dynamic mechanical characterization of polypropylene-woodflourcomposites. *Polym. Eng. Sci.* **2002**, *42*, 733−742.
(16) Rosa, M. F.; Chiou, B. S.; Medeiros, E. S.; Wood, D. F.; Williams, T. G.; Mattoso, L. H. C.; Orts, W. J.; Imam, S. H. Effect of fiber treatments on tensile and thermal properties of starch/ethylene vinyl alcohol copolymers/coir biocomposites. *Bioresour. Technol.* **2009**, *100*, 5196−5202.
(17) Pickering, K. L.; Efendy, M. A.; Le, T. M. A review of recent developments in natural fibre composites and their mechanical performance. *Composites, Part A* **2016**, *83*, 98−112.
(18) Mahesha, G. T.; Shenoy, S. B.; Kini, V. M.; Padmaraja, N. H. Effect of fiber treatments on mechanical properties of Grewia serrulata bast fiber reinforced polyester composites. *Mater. Today Proc.* **2018**, *5*, 138−144.
(19) Shah, A. H.; Li, X.; Xu, X. D.; Dayo, A. Q.; Liu, W. B.; Bai, J. W.; Wang, J. Evaluation of mechanical and thermal properties of modified epoxy resin by using acacia catechu particles. *Mater. Chem. Phys.* **2019**, *225*, 239−246.
(20) Wan, T.; Huang, R. Q.; Zhao, Q. H.; Xiong, L.; Qin, L. L.; Tan, X. M.; Cai, G. J. Synthesis of wheat straw composite superabsorbent. *J. Appl. Polym. Sci.* **2013**, *130*, 3404−3410.
(21) Wang, Z. X.; Barford, J. P.; Hui, C. W.; Mckay, G. Kinetic and equilibrium studies of hydrophilic and hydrophobic rice husk cellulosic fibers used as oil spill sorbents. *Chem. Eng. J.* **2015**, *281*, 961−969.
(22) Dorris, G. M.; Gray, D. G. Adsorption of n-alkanes at zero surface coverage on cellulose paper and wood fibers. *J. Colloid Interface Sci.* **1980**, *77*, 353−362.
(23) Wang, J. T.; Zheng, Y.; Wang, A. Q. Coated kapok fiber for removal of spilled oil. *Mar. Pollut. Bull.* **2013**, *69*, 91−96.
(24) Zuo, Y. F.; Gu, J. Y.; Yang, L.; Qiao, Z. B.; Tan, H. Y.; Zhang, Y. H. Synthesis and characterization of maleic anhydride esterified corn starch by the dry method. *Int. J. Biol. Macromol.* **2013**, *62*, 241−247.
(25) Wang, F.; Zhou, S. J.; Li, L.; Zhang, X. P. Changes in the morphological−mechanical properties and thermal stability of bamboo fibers during the processing of alkaline treatment. *Polym. Composite.* **2018**, *39*, E1421−E1428.
(26) Wang, X.; Song, L.; Yang, H. Y.; Xing, W. Y.; Kandola, B.; Hu, Y. Simultaneous reduction and surface functionalization of graphene oxide with POSS for reducing fire hazards in epoxy composites. *J. Mater. Chem.* **2012**, *22*, 22037−22043.
(27) Wang, J. L.; Ma, C.; Wang, P. L.; Qiu, S. L.; Cai, W.; Hu, Y. Ultra-low phosphorus loading to achieve the superior flame retardancy of epoxy resin. *Polym. Degrad. Stab.* **2018**, *149*, 119−128.
(28) Zhou, K. Q.; Jiang, S. H.; Bao, C. L.; Song, L.; Wang, B. B.; Tang, G.; Hu, Y.; Gui, Z. Preparation of poly (vinyl alcohol) nanocomposites with molybdenum disulfide (MoS 2): structural characteristics and markedly enhanced properties. *RSC Adv.* **2012**, *2*, 11695−11703.
(29) Farkas, A.; Strohm, P. F. Imidazole catalysis in the curing of epoxy resins. *J. Appl. Polym. Sci.* **1968**, *12*, 159−168.
(30) Dominguez, J. C.; Grivel, J. C.; Madsen, B. Study on the non-isothermal curing kinetics of a polyfurfuryl alcohol bioresin by DSC using different amounts of catalyst. *Thermochim. Acta* **2012**, *529*, 29−35.
(31) Barton, J. M. The application of differential scanning calorimetry (DSC) to the study of epoxy resin curing reactions. *Adv. Polym. Sci.* **1985**, *72*, 111−154.
(32) Yang, K.; Ritchie, R. O.; Gu, Y. Z.; Wu, S. J.; Guan, J. High volume-fraction silk fabric reinforcements can improve the key mechanical properties of epoxy resin composites. *Mater. Design.* **2016**, *108*, 470−478.
(33) Naznin, M.; Abedin, M. Z.; Khan, M. A.; Gafur, M. A. *Influence of Acacia Catechu Extracts and Urea and Gamma Irradiation on the Mechanical Properties of Starch/PVA-based Material*; International Scholarly Research Network ISRN Polymer Science 2012, 2012; p 348685.
(34) Balan, A. K.; Mottakkunnu Parambil, S.; Vakyath, S.; Thulissery Velayudhan, J.; Naduparambath, S.; Etathil, P. Coconut shell powder reinforced thermoplastic polyurethane/natural rubber blend-composites: effect of silane coupling agents on the mechanical and thermal properties of the composites. *J. Mater. Sci.* **2017**, *52*, 6712−6725.
(35) Zhang, Y.; Choi, J. R.; Park, S. J. Thermal conductivity and thermo-physical properties of nanodiamond-attached exfoliated hexagonal boron nitride/epoxy nanocomposites for microelectronics. *Composites, Part A* **2017**, *101*, 227−236.
(36) Zainuddin, S.; Fahim, A.; Arifin, T.; Hosur, M. V.; Rahman, M. M.; Tyson, J. D.; Jeelani, S. Optimization of mechanical and thermo-mechanical properties of epoxy and E-glass/epoxy composites using NH2-MWCNTs, acetone solvent and combined dispersion methods. *Compos. Struct.* **2014**, *110*, 39−50.
(37) Goertzen, W. K.; Kessler, M. R. Dynamic mechanical analysis of carbon/epoxy composites for structural pipeline repair. *Compos. B Eng.* **2007**, *38*, 1−9.
(38) Saha, A. K.; Das, S.; Bhatta, D.; Mitra, B. C. Study of jute fiber reinforced polyester composites by dynamic mechanical analysis. *J. Appl. Polym. Sci.* **1999**, *71*, 1505−1513.
(39) Pothan, L. A.; Thomas, S.; Groeninckx, G. The role of fibre/matrix interactions on the dynamic mechanical properties of chemically modified banana fibre/polyester composites. *Composites, Part A* **2006**, *37*, 1260−1269.
(40) Hornsby, P. R.; Hinrichsen, E.; Tarverdi, K. Preparation and properties of polypropylene composites reinforced with wheat and flax straw fibres: part I fibre characterization. *J. Mater. Sci.* **1997**, *32*, 443−449.
(41) Mohammed, A. A. B. A.; Hasan, Z.; Omran, A. A. B.; Kumar, V. V.; Elfaghi, A. M.; Ilyas, R. A.; Sapuan, S. M. Corn: Its Structure, Polymer, Fiber, Composite, Properties, and Applications. *Polymers* **2022**, *14*, 4396.

https://doi.org/10.1021/acsomega.2c06947
ACS Omega 2023, 8, 12644−12652